Research Article Vol. 2, No. 3 / 15 March 2019 / OSA Continuum 983

Two-photon fluorescence laser sheet imaging for high contrast visualization of atomizing sprays

EDOUARD BERROCAL,[1,*] CHRIS CONRAD,[2] JEREMIAS PÜLS,[1] CORD L. ARNOLD,[3] MICHAEL WENSING,[2] MARK LINNE,[4] AND MIGUEL MIRANDA[3,5]

[1] *Division of Combustion Physics, Department of Physics, Lund University, Lund, Sweden*
[2] *Lehrstuhl für Technische Thermodynamik, Friedrich-Alexander Universität Erlangen-Nürnberg, Erlangen, Germany*
[3] *Division of Atomic Physics, Department of Physics, Lund University, Lund, Sweden*
[4] *Institute for Multiscale Thermofluids, School of Engineering, University of Edinburgh, UK*
[5] *IFIMUP-IN and Departamento de Física e Astronomia,Universidade do Porto, Portugal*
[*] *edouard.berrocal@forbrf.lth.se*

Abstract: Two-photon excitation laser induced fluorescence (2p-LIF) is used here for imaging an optically dense atomizing spray. The main advantage of the approach is that very little fluorescence interference originating from multiple light scattering is generated. This leads to high image contrast and a faithful description of the imaged fluid structures. While point measurement 2p-LIF imaging is a well-known approach used in life science microscopy, it has, to the best of the authors' knowledge, never been tested for analyzing liquid structures in spray systems. We take advantage of this process, here, at a macroscopic scale (~ 5 × 5 mm field of view) by imaging the central part of a light sheet of 10 mm height. To generate enough 2p-LIF signal at such a scale and with single-shot detection, ultra-short laser pulses of 25 fs, centered at 800 nm wavelength and having 2.5 mJ pulse energy, have been used. The technique is demonstrated by imaging a single spray plume from a 6 hole commercial Gasoline Direct Injection (GDI) system running at 200 bar injection pressure. The proposed approach is very promising for detailed analysis of liquid breakups in optically dense sprays and can be used for other fluid mechanics related applications.

1. Introduction

Spray systems are ubiquitous; they are used for painting, cooling, misting, washing, applying chemicals, dispersing liquids, material processing *etc*. Nevertheless, the most significant spray application concerns the injection of liquid fuel into combustion engines. Internal combustion and gas turbines engines are two very important examples of devices which provide mechanical power using most often a liquid fuel spray. Due to pressure for efficiency improvement and reduced pollutant emission, interest in the fuel-injection process has grown during the last couple of decades. However, imaging atomizing sprays is extremely challenging due to the lack of visibility. Most often, the light intensity fraction of the non-scattered photons ranges from 13.5% down to 0.01%. In simple terms of visibility, this level of light transmission corresponds to the transition between seeing a blurred object to not seeing it at all. In such situations a very large amount of the detected light intensity originates from photons that have been scattered multiple times; directly concealing spray features which could reveal the dynamic of spray formation.

To overcome problems related to multiple light scattering, the experimental development of advanced imaging techniques and the means employed for the characterization of optically dense sprays has increased during the past decade [1–3]. Three main imaging approaches in

#346903 https://doi.org/10.1364/OSAC.2.000983
Journal © 2019 Received 27 Sep 2018; accepted 15 Jan 2019; published 13 Mar 2019

OSA CONTINUUM

which multiple light scattering can be mitigated currently exist: Ballistic Imaging (BI) [4], X-ray imaging [5] and Structured Laser Illumination Planar Imaging (SLIPI) [6,7]. X-ray imaging and BI are usually employed in the near field spray region, close to the injector tip, where relatively large liquid structures are present. Thanks to its light sheet configuration, SLIPI provides sectioned images [8] and is most often employed to characterize clouds of already formed micrometric droplets located in the spray region. However, when applying SLIPI near the nozzle tip, corresponding to the spray formation region, the incident modulated line structures are vanished due to refraction at the liquid/air interfaces. Those effects restrict the SLIPI technique to probe micrometric liquid droplets of size much smaller than the spatial period of the modulated light sheet.

Microscopic high-speed imaging is now a popular approach for spray diagnostics, thanks to the recent development of high-speed cameras and high quality long range microscope objectives. It has been successfully applied to the study of Diesel sprays as shown in [9]. However, those high resolution spray images are usually recorded on a shadowgraphy configuration without optical sectioning advantages.

It has been recently demonstrated in [10] that Light Sheet Fluorescence Microscopy (LSFM) provides valuable spray information while elastic scattering is not faithful to the liquid structures. This is due to the fact that elastically scattered light is generated at the liquid/gas interfaces and a collimated beam will have light reflected and refracted to some preferential directions due to those boundaries. This creates a number of unwanted artifacts such as glare points and strong reflections responsible to saturation spots on the recorded images as shown in [10]. Conversely, the LIF signal generated within the liquid is mostly volume dependent and shows faithful images of the liquid structures.

Despite the advantages of LSFM for imaging the spray formation region, the approach remains affected by multiple light scattering. There is, thus, an important need in developing a light sheet imaging approach where high-contrast images of the spray formation region can be obtained from single-shot recordings.

In this article, we propose the possibility of using a two-photon excitation scheme [11], instead of single-photon excitation. The advantage of 2p-LIF detection is that it provides higher visibility through turbid media. The main reason for this is that photons which undergo multiple scattering processes spread in space and time, making the probability of having two photon simultaneously absorbed highly reduced. On the contrary, at the location where the illuminating light sheet is focused the probability for the 2p-LIF process to occur at its highest; providing a signal that is only generated at the object plane of the camera objective. The efficiency of the approach is tested, here, on a 6 hole commercial GDI spray system operating at 200 bar injection pressure and for 200 µs after the visible start of the injection. To assess the image contrast enhancement and the benefits of two-photon fluorescence light sheet imaging for visualization within atomizing sprays, an image comparison is performed for various detection schemes:

1) Shadowgraphy imaging, 2) Laser sheet elastic scattering, 3) Laser sheet one-photon fluorescence, 4) Laser sheet two-photon fluorescence.

2. Two-photon excitation

Two-photon absorption or excitation is a nonlinear process that was theoretically derived by Maria Göppert-Mayer in 1931 and later experimentally proven after the invention of the laser [12]. Electrons within an atom are excited from the ground state to an excited state by incoming photons, on the condition that the energy of the photon matches the difference in energy between two quantum states. If the light intensity is sufficiently high, also two-photon excitation can happen simultaneously, where the combined energy of the two photons matches the energy requirement; this event is called two-photon excitation. When illuminating a homogeneous liquid volume containing fluorescing molecules, the signal generated by single-photon fluorescence, as

OSA CONTINUUM

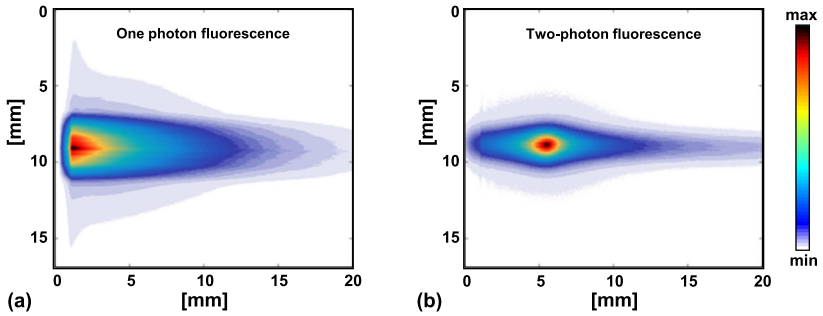

Fig. 1. Comparison between single-photon (a) and two-photon (b) excitation processes for a beam crossing a water solution containing diluted fluorescein dye. In (a), the dye is excited at 450 nm using a CW diode laser. In (b) femtosecond pulses generated by a titanium-sapphire femtosecond laser are used to excite the water solution. In this example the incident beam is focused by a cylindrical lens of +50 mm focal length.

shown in Fig. 1(a), is exponentially reduced with distance. This light intensity reduction along the path length x is described by the Beer-Lambert law:

$$I(x) = I_0 \cdot e^{-N \cdot \sigma_a \cdot x} \tag{1}$$

where I_0 is the incident light intensity, N is the number density of the dye molecules and σ_a is the single-photon absorption cross-section. However, for two-photon absorption, the generated fluorescence differs fundamentally from single-photon absorption and is described as:

$$I(x) = \frac{I_0}{1 + N \cdot \delta \cdot x \cdot I_0} \tag{2}$$

where δ is the molecular two-photon cross-section quoted in the units of Göppert-Mayer (GM). By definition, 1 GM = 10 - 50 cm^4 s $photon^{-1}$, corresponding to the product of the cross-sections, in cm^2, from each photon. Note that the focal distance of a focusing lens plays an important role in the case of two-photon fluorescence, as the energy density varies with location. This directly affects the 2p-LIF signal with distance depending on the focal length, as shown in Fig. 2.

It is worth noting that two-photon laser induced fluorescence has been reported in the combustion literature to detect species that are not accessible to one-photon excitation (e.g. CO in Refs. [13,14]). The molecular work mitigates spectroscopic and interference issues associated with 2p-LIF in gaseous flames that have no scatters present. The current article seeds a dye into liquid and demonstrates how 2p-LIF can be used in a scattering environment

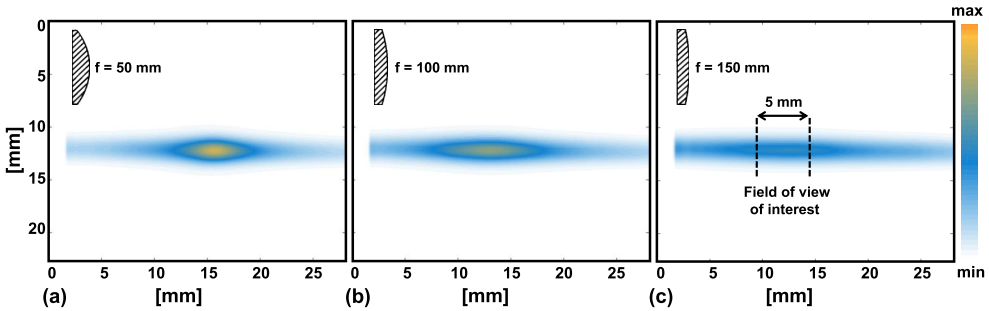

Fig. 2. Effect of the focal distance of a converging cylindrical lens on the generation of two-photon excitation fluorescence signal. Here, the focal distance corresponds to 50 mm, 100 mm and 150 mm in (a), (b) and (c) respectively. By using longer focal distances a more homogeneous two-photon fluorescence signal is generated.

OSA CONTINUUM

to mitigate image corruption caused my multiple scattering of the input laser light. The two topics are entirely different but complementary. Fluorescence signals collected from two-phase flow systems are commonly generated from single-photon excitation. However, under certain conditions, they can also be generated from two-photon excitation. In this case the energy density of the incident beam is an important parameter to increase the probability that two photons get absorbed simultaneously. Therefore, ultra-short laser pulses (e.g. $\sim$ 80 femtosecond duration) are usually used to induce this process. The main advantage of this scheme, is that the Mie multiple light scattering - from the surrounding spherical droplets - does not provide sufficiently high intensity to induce a two-photon absorption process. As a result, a large portion of undesired signal, as illustrated in Fig. 3(b), is not generated with two-photon excitation, leading to visibility

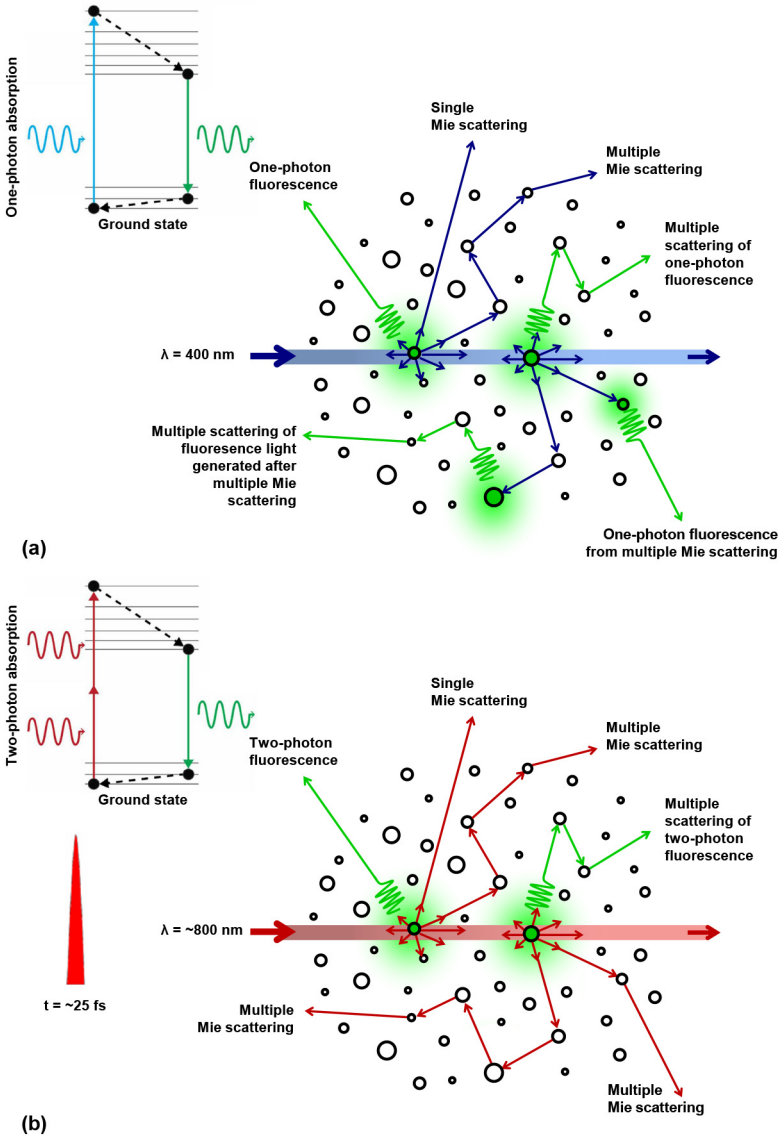

Fig. 3. Comparison between (a) single-photon and (b) two-photon excitation processes applied in a spray system consisting of a cloud of droplets. The fluorescence from two-photon excitation is only generated along the light sheet reducing a significant part of unwanted fluorescence outside of the light sheet.

OSA CONTINUUM

enhancement. A second advantage is the possibility to focus sharply the incident light sheet to induce locally a signal. A third advantage is the possibility to counter balance the effects of light extinction along the incident path of the laser beam, once again by adequately focusing the incident beam.

3. Experiment

The laser system used here is a titanium-sapphire chirped pulse amplification femtosecond system, delivering pulses at 1 kHz repetition rate with 800 nm central wavelength. The light pulses have 2.5 mJ of energy and a duration of 25 fs which has been measured in the region of interest, below the nozzle tip, using the d-scan technique [15]. The injected liquid is a solution of water with fluorescein dye - 40 mL solution of dye concentrated at 7% by weight within 2400mL water. This results in a weight ratio of $\sim 1/1000$ fluorescein, which does not affect the surface tension nor the density of the injected water. The pH of the solution was ~ 7. In terms of two-photon excitation in spray systems, the choice of fluorescein dye presents several advantages:

1) The absorption spectrum for two-photon excitation [16] matches well the femtosecond pulse excitation used here. 2) The quantum yield of fluorescein emission in water is very high (>0.9 depending on the pH). 3) It is a non-toxic organic dye, which is highly soluble in water. 4) The fluorescence lifetime of fluorescein is in the range of $\sim$ 4ns, freezing the motion of the injected liquid.

When generating one-photon fluorescence, a frequency-doubling BBO crystal is inserted in the illumination path, producing an excitation pulse of 400 nm wavelength. To record the fluorescence signal from both excitation schemes, a band-pass filter centered at 510 nm with 90 nm bandwidth is used in front of the camera objective. To efficiently suppress the scattered light, the filter has a blocking optical density larger than 6. The spectra of the excitation pulses as well as of the fluorescence signal are given in Fig. 4. The aqueous fluorescein solution is injected at 200 bar pressure into ambient temperature and pressure conditions. Two alternative hydraulic intensifiers are used to keep the pressure of the working fluid stable during injection. Only one spray plume is illuminated with the light sheet. The imaging system consists of a telecentric lens objective (Gold TL from Edmund Optics of $\times 1$ primary magnification with more than 50%image contrast at 40 lp/mm) used at F# 6 and mounted on a 14 bit CCD camera (Luca R from Andor - 1002×1004 pixels) resulting to 5 microns per pixel.

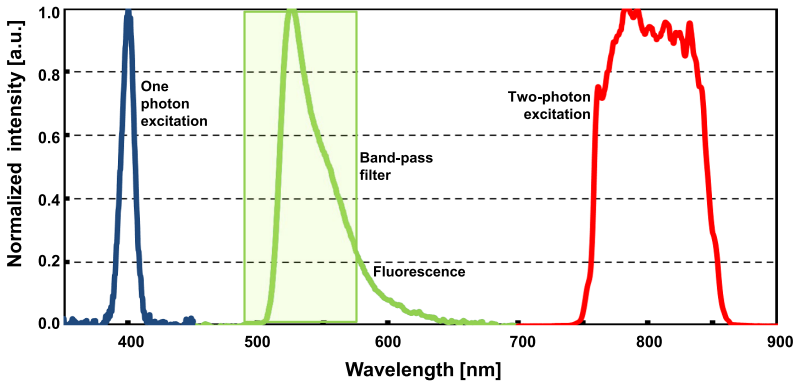

Fig. 4. Spectra of the one-photon excitation at 400 nm, the fuorescein emission and the two-photon excitation centered at 800 nm. To generate the 400 nm excitation pulse, the 800 nm laser beam is frequency doubled by inserting a BBO crystal.

To generate a shadow image, a fluorescing screen is illuminated at the back of the spray as shown in Fig. 5(a). To create a light sheet for the 2p-LIF, Fig. 5(b), a positive cylindrical lens of

OSA CONTINUUM

150 mm length focal is used. This distance allows to generate a homogeneous light sheet signal over the field of view as seen in Fig. 2(c). For the the elastic scattering detection illustrated in Fig. 5(c) the signal is obtained by simply removing the fluorescence band-pass filter in front of the camera and injecting water without adding any fluorescing dye. For the 1p-LIF detection, Fig. 5(d), a BBO crystal is positioned in the beam path, doubling the frequency of the incident wavelength.

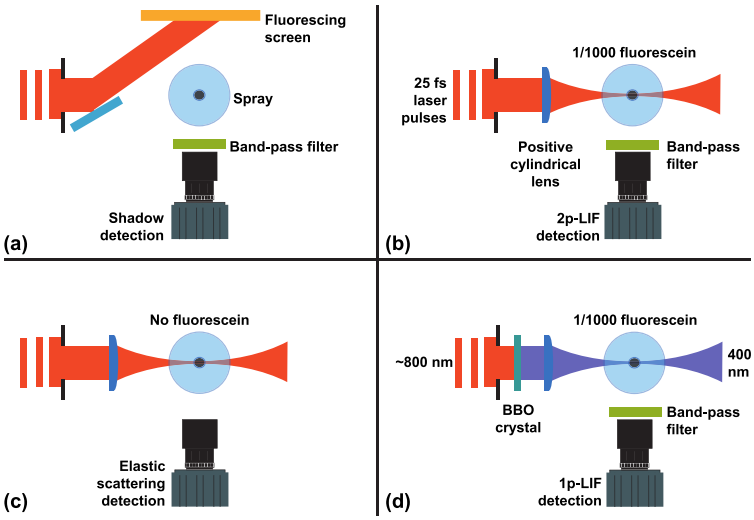

Fig. 5. Description of the optical arrangement for each detection configuration. The detection corresponding to shadowgraphy imaging, two-photon fluorescence, elastic light scattering and one-photon fluorescence are shown in (a), (b), (c) and (d) respectively.

It should be noted that the detection system - camera and objective - as well as the spray injection characteristics - pressure of injection and recording time after the visible start of injection - have been kept exactly the same while transiting from one detection scheme to another. This approach did allow to make results comparable in terms of amount of optical signal, image contrast and pixel resolution.

4. Results and discussion

One important aspect is to determine the benefits of 2p-LIF laser sheet imaging by comparing it with other detection schemes such as shadowgraphy, laser sheet light scattering and laser sheet 1p-LIF. The optical arrangement of each of those detection scheme is given in Fig. 5 In order to make this comparison as rigorous as possible, each imaging case is based on the same detection system and the spray was running under identical conditions. In addition, no post-processing apart of the camera noise subtraction have been applied to the presented images.

The first image results comparison concerns shadowgraphy and 2p-LIF light sheet imaging and is given in Fig. 6. Due to its line-of-sight configuration, the shadowgraph image is strongly affected by the presence liquid structures and droplets located outside the image plane of the camera lens. Thus, one apparent observation is the presence of a large dark area on the right side of the imaged spray plume in (a) depicting the the presence of the other spray plumes. This effect is commonly referred in the literature related to atomizing spray as obscuration and is induced by the extinction of light by the droplets located along the path between the light source and the camera lens. For the case of 2p-LIF, shown in (b), the 5 other out-of-focus spray plumes are not visible and only the desired spray plume is imaged. The suppression of this unwanted contribution

OSA CONTINUUM

can be explained by two reasons: 1) The use of a light sheet which provides an illuminated section of the spray; defined as optical sectioning. 2) The use of two-photon fluorescence which is generated only where the light sheet remains focused. Thus, the surrounding light generated by scattering, do not have enough energy to induce a 2p-fluorescence signal. It is also seen from the ×2 zoom areas that the image contrast of the liquid structures is strongly affected in Fig. 6(a) but not in Fig. 6(b). Thus, for the case of 2p-LIF, the unconnected liquid structures, the blobs, the droplets and voids are clearly visible.

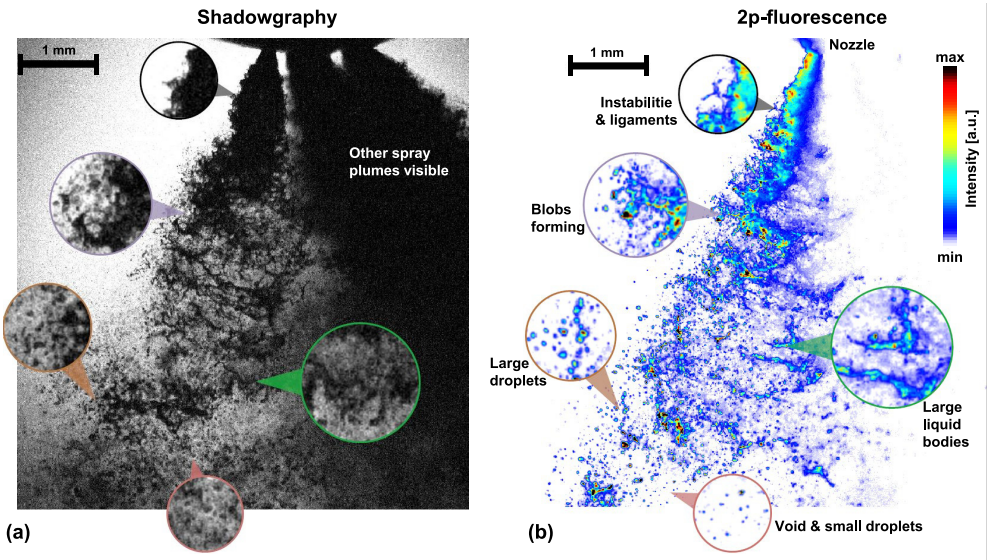

Fig. 6. Image results comparison between shadowgraphy in (a) and 2p-LIF light sheet imaging in (b) for a 6 holes GDI spray injected at 200 bars liquid pressure and recorded at 200 µs. The two images have been recorded with the exact same camera system and operating conditions. While the shadowgraph image shows blurred liquid structures; the droplets, liquid blobs, ligaments and voids are clearly observable in the ×2 zoomed areas of the 2p-LIF image.

In the second image results comparison, given in Fig. 7, two light sheet imaging illumination are now compared, one for the detection of elastic light scattering in (a) and one for the detection of 2p-LIF in (b). It is seen that despite the light sheet configuration, large amount of background light remains generated by the 5 other out-of-focus spray plumes for the case of the elastics scattering detection. This light intensity contribution is the results of multiple light scattering. Similarly to the previous comparison case, the 2p-LIF image provides high contrast image of the desired spray plume only. This indicates that light scattering, located outside from the imaged light sheet does not generate any 2p-fluorescence signal.

It is seen from the ×3 zoomed areas of Fig. 7 that the liquid structures located inside the spray formation region cannot be observed with the elastic scattering detection. In contrast, the 2p-LIF signal, reveals formerly hidden liquid structures.

As explained previously, the elastically scattered light is generated at the liquid/gas interfaces. Thus, in some situation, the shape of irregular liquid structures will reflect or refract light directly into the objective lens, locally saturating the camera sensor. Those peaks of saturated signals can be seen from the optical signals given in Fig. 8. In this figure, an elongate small area of 83 µm and 1.25 mm long and located at 4 mm down and 1.5 mm side from the nozzle orifice is selected. Three different injection events are shown for both elastic scattering and 2p-LIF detection. The peaks of light intensity from the elastic light scattering are evident from those

OSA CONTINUUM

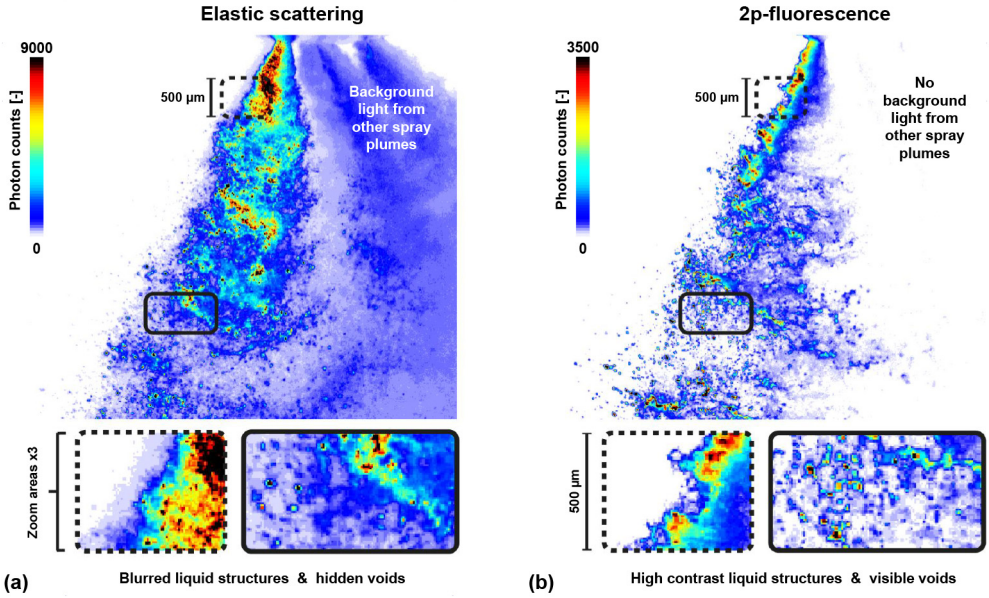

Fig. 7. Light sheet imaging comparison between elastic scattering in (a) and 2p-LIF light sheet imaging in (b) for the 6 holes GDI spray injected at 200 bars liquid pressure and recorded at 200 µs. The two images have been recorded with the same camera system but corresponds to independent injection events. It is seen from the ×3 zoom areas that 2p-LIF provides images with limited blur allowing the visibility of liquid structures which are not observable with the elastic scattering scattering scheme.

examples. Thus, by default, the elastic light scattering from a collimated light sheet is not faithful to the imaged liquid bodies, especially when irregular elements are present. Conversely, the LIF signal is volume dependent and provides faithful images of the shape of imaged liquid elements.

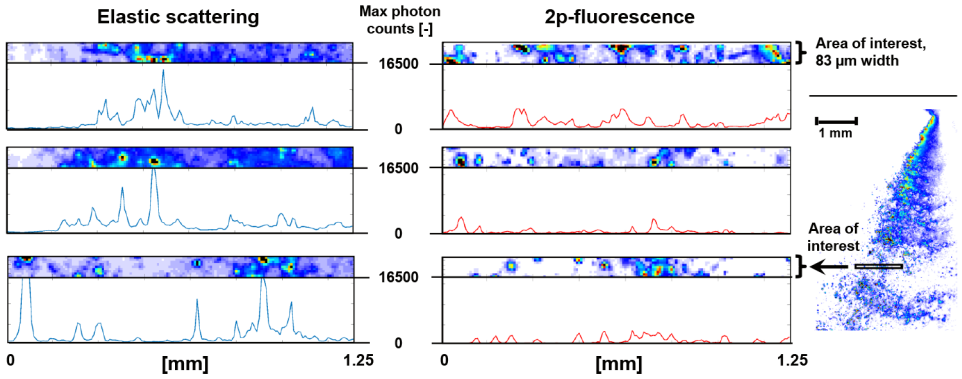

Fig. 8. Optical signals comparison between elastic scattering and 2p-LIF light sheet imaging. The area of interest is located at 4 mm below the nozzle tip as shown in the image on the right. Each image corresponds to independent injection events. It is observed here that the Mie scattering image is locally affected by strong reflections that saturate the 14 bit camera. On the contrary the 2p-LIF signal does not show those unwanted intensity peaks.

OSA CONTINUUM

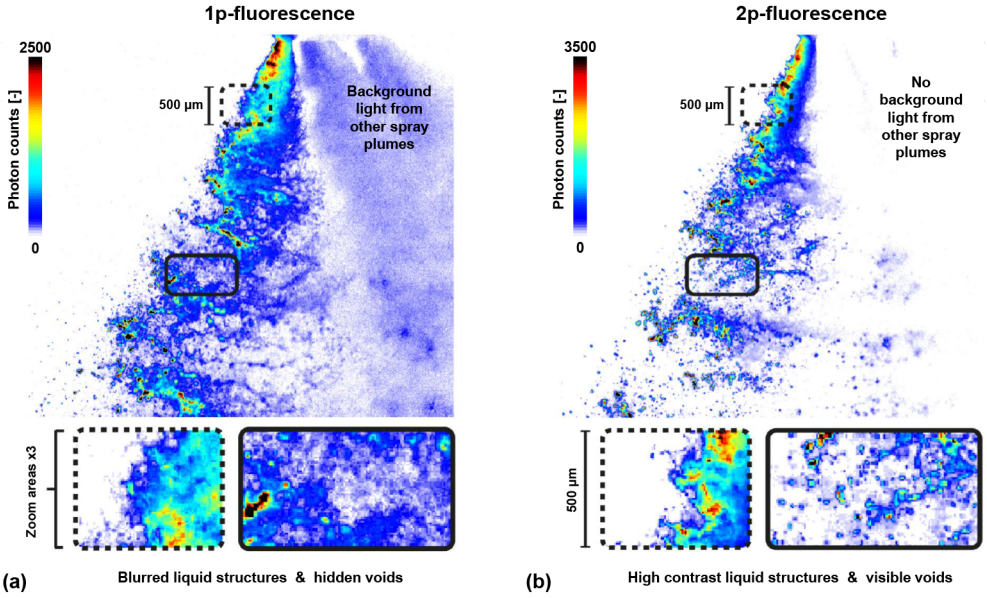

Fig. 9. Light sheet imaging comparison between 1p-LIF in (a) and 2p-LIF light sheet imaging in (b) for the 6 holes GDI spray injected at 200 bars liquid pressure and recorded at 200 µs. The two images have been recorded with the same camera system but corresponds to independent injection events. It is seen from the ×3 zoom areas that 2p-LIF provides images with limited blur allowing the visibility of liquid structures which are not observable with the 1p-LIF scheme.

The last image results comparison is given in Fig. 9, where two light sheet imaging from liquid LIF are compared: one for the detection of 1p-LIF in (a) and one for the detection of 2p-LIF in (b). Even though less apparent than for the two previous detection schemes, it is also observed that the out-of-focus spray plumes are visible for the case of 1p-LIF. This is the results of the

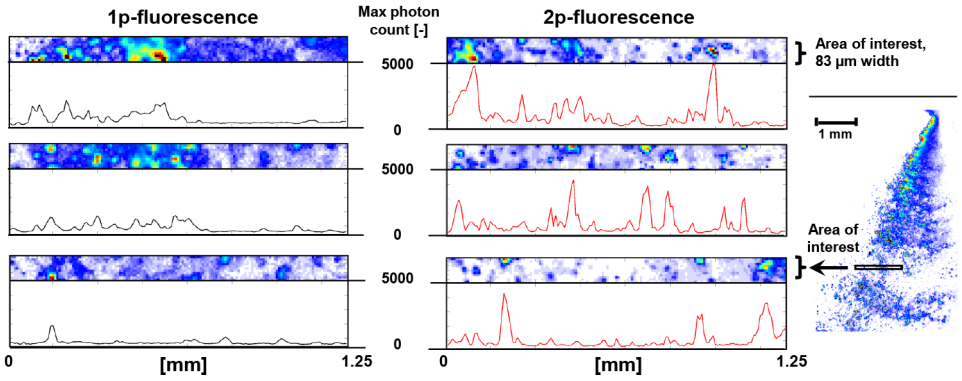

Fig. 10. Optical signals comparison between 1p-LIF and 2p-LIF light sheet imaging. The area of interest is located at 4 mm below the nozzle tip as shown in the image on the right. Each image corresponds to independent injection events. It is observed here that the 1p-LIF does not show high contrast signal levels between the imaged droplets and their surrounding. On the contrary the 2p-LIF signal is strongly increased where droplets are imaged, indicating clearly their presence.

OSA CONTINUUM

multiply scattered photons that induce a 1p-LIF signal, but do not a 2p-LIF signal. Once again, it is seen from the ×3 zoomed areas of Fig. 9 that the liquid structures located inside the spray formation region cannot always be observed from the 1p-LIF signal while the 2p-LIF signal reveals formerly hidden liquid structures.

When analyzing the optical signals, shown in Fig. 10, it is observed that the 2p-LIF shows much stronger signal variations at locations of the imaged droplets; still without the saturation effects observed with the elastic scattering. However, the 1p-LIF signals have smoother variations which result to a lower image contrast.

Finally, it can be noted that along the light sheet, photons are scattered and deflected mostly in the forward direction by the micrometric droplets. This results to an increase the light sheet thickness with distance (light sheet broadening). However, 2p-LIF can only be generated where the focus of the light sheet remains sufficiently sharp with enough energy. This specificity provides a better spatial sectioning with the two-photon approach, outperforming both the elastic scattering and 1p-LIF.

5. Conclusion

In conclusion, we have described in this paper a demonstration of two-photon planar laser induced fluorescence imaging for time-resolved single shot, high-resolution imaging in sprays. Perhaps the most significant advantage of this technique is the fact that multiple light scattering of the excitation laser beam does not generate an interfering fluorescence signal. The technique thus provides high fidelity images of ligaments and drops during spray formation. The necessary laser source for such a measurement has become commercially available, rendering the technique usable in many different labs. Continuing work will evaluate and extend the technique for the study of spray dynamics by tracking over time the individual liquid structures. Another future work will consist in quantifying the image contrast enhancement in controlled scattering environments, by using dyed polystyrene spheres of known size and concentration, similar to the work presented in [17]. Finally, two-photon light sheet imaging is very promising for visualization in challenging fuel injection spray systems and can be used in the future to generate experimental data for the validation of spray breakups models.

Funding

H2020 European Research Council (ERC) (638546); Fundação para a Ciência e a Tecnologia (FCT) (Network of Extreme Conditions Laboratories—NECL, NORTE-01-0145-FEDER-022096); Vetenskapsrådet (VR) (2016-03894).

References

1. A. Coghe and G. Cossali, "Quantitative optical techniques for dense sprays investigation: A survey," Opt. Lasers Eng. **50**(1), 46–56 (2012). Advances in Flow Visualization.
2. M. Linne, "Imaging in the optically dense regions of a spray: A review of developing techniques," Prog. Energy Combust. Sci. **39**(5), 403–440 (2013).
3. T. D. Fansler and S. E. Parrish, "Spray measurement technology: a review," Meas. Sci. Technol. **26**(1), 012002 (2015).
4. M. A. Linne, M. Paciaroni, E. Berrocal, and D. Sedarsky, "Ballistic imaging of liquid breakup processes in dense sprays," Proc. Combust. Inst. **32**(2), 2147–2161 (2009).
5. C. F. Powell, S. A. Ciatti, S.-K. Cheong, J. Liu, and J. Wang, "X-ray absorption measurements of diesel sprays and the effects of nozzle geometry," *SAE Technical Paper*, (SAE International, 2004).
6. E. Berrocal, E. Kristensson, M. Richter, M. Linne, and M. Aldén, "Application of structured illumination for multiple scattering suppression in planar laser imaging of dense sprays," Opt. Express **16**(22), 17870–17881 (2008).
7. E. Kristensson and E. Berrocal, "Crossed patterned structured illumination for the analysis and velocimetry of transient turbid media," Sci. Rep. **8**(1), 11751 (2018).
8. Y. N. Mishra, E. Kristensson, M. Koegl, J. Jönsson, L. Zigan, and E. Berrocal, "Comparison between two-phase and one-phase slipi for instantaneous imaging of transient sprays," Exp. Fluids **58**(9), 110 (2017).

OSA CONTINUUM

9. C. Crua, M. R. Heikal, and M. R. Gold, "Microscopic imaging of the initial stage of diesel spray formation," Fuel **157**, 140–150 (2015).
10. E. Berrocal, E. Kristensson, and L. Zigan, "Light sheet fluorescence microscopic imaging for high-resolution visualization of spray dynamics," Int. J. Spray Combust. Dyn. **10**(1), 86–98 (2018).
11. P. T. So, Two-photon Fluorescence Light Microscopy (American Cancer Society, 2001).
12. M. Pawlicki, H. A. Collins, R. G. Denning, and H. L. Anderson, "Two-photon absorption and the design of two-photon dyes," Angew. Chem., Int. Ed. **48**(18), 3244–3266 (2009).
13. D. R. Richardson, S. Roy, and J. R. Gord, "Femtosecond, two-photon, planar laser-induced fluorescence of carbon monoxide in flames," Opt. Lett. **42**(4), 875–878 (2017).
14. Y. Wang, A. Jain, and W. Kulatilaka, "CO imaging in piloted liquid-spray flames using femtosecond two-photon LIF," *Proc. Combust. Inst.* (2018).
15. M. Miranda, T. Fordell, C. Arnold, A. L'Huillier, and H. Crespo, "Simultaneous compression and characterization of ultrashort laser pulses using chirped mirrors and glass wedges," Opt. Express **20**(1), 688–697 (2012).
16. C. Xu, W. Zipfel, J. B. Shear, R. M. Williams, and W. W. Webb, "Multiphoton fluorescence excitation: new spectral windows for biological nonlinear microscopy," Proc. Natl. Acad. Sci. USA **93**(20), 10763–10768 (1996).
17. M. Gu, S. P. Schilders, and X. Gan, "Two-photon fluorescence imaging of microspheres embedded in turbid media," J. Mod. Opt. **47**(6), 959–965 (2000).